Dangling-bond spin relaxation and magnetic $1/f$ noise from the amorphous-semiconductor/oxide interface: Theory

Rogerio de Sousa*
Department of Physics, University of California, Berkeley, California 94720, USA
(Received 28 May 2007; revised manuscript received 18 September 2007; published 6 December 2007)

We propose a model for magnetic noise based on spin flips (not electron trapping) of paramagnetic dangling bonds at the amorphous-semiconductor/oxide interface. A wide distribution of spin-flip times is derived from the single-phonon cross-relaxation mechanism for a dangling bond interacting with the tunneling two-level systems of the amorphous interface. The temperature and frequency dependence is sensitive to three energy scales: The dangling-bond spin Zeeman energy (δ), as well as the minimum ($E_{\min}$) and maximum ($E_{\max}$) values for the energy splittings of the tunneling two-level systems. At the highest temperatures, $k_BT \gg \max(\delta, E_{\max})$, the noise spectral density is independent of temperature and has a $1/f$ frequency dependence. At intermediate temperatures, $k_BT \gg \delta$ and $E_{\min} \ll k_BT \ll E_{\max}$, the noise is proportional to a power law in temperature and possesses a $1/f^p$ spectral density, with $p=1.2-1.5$. At the lowest temperatures, $k_BT \ll \delta$, or $k_BT \ll E_{\min}$, the magnetic noise is exponentially suppressed. We compare and fit our model parameters to a recent experiment probing spin coherence of antimony donors implanted in nuclear-spin-free silicon [T. Schenkel *et al.*, Appl. Phys. Lett. **88**, 112101 (2006)], and conclude that a dangling-bond area density of the order of 10^{14} cm^{-2} is consistent with the data. This enables the prediction of single spin qubit coherence times as a function of the distance from the interface and the dangling-bond area density in a real device structure. We apply our theory to calculations of magnetic flux noise affecting superconducting quantum interference devices (SQUIDs) due to their Si/SiO_2 substrate. Our explicit estimates of flux noise in SQUIDs lead to a noise spectral density of the order of $10^{-12}\ \Phi_0^2(\mathrm{Hz})^{-1}$ at $f=1$ Hz. This value might explain the origin of flux noise in some SQUIDs. Finally, we consider the suppression of these effects using surface passivation with hydrogen, and the residual nuclear-spin noise resulting from a perfect silicon-hydride surface.

DOI: 10.1103/PhysRevB.76.245306 PACS number(s): 73.50.Td, 61.43.−j, 76.30.−v, 85.25.Dq

I. INTRODUCTION

Our physical understanding of spin relaxation in semiconductors plays a crucial role in the current development of spin-based electronics[1] and spin-based quantum computation.[2] One question that received little or no attention so far is related to magnetic noise in semiconductor devices and nanostructures. Magnetic noise from impurities and other defects at the interface may be the dominant source of spin phase relaxation (decoherence) for implanted donor electrons[3] or nuclear spins[4] in isotopically purified silicon. Moreover, because Si/SiO_2 and other amorphous oxide interfaces are used as the substrate for sensitive superconducting quantum interference device (SQUID) magnetometers,[5–7] the spin relaxation of magnetic impurities at the substrate might explain the observed magnetic flux noise in these devices.

One universal characteristic of silicon devices is the presence of an insulating interface, usually an oxide, separating the metallic gate from the semiconductor. It is known for a long time that these interfaces are rich in dangling-bond-type defects (also denoted "P_b centers") which can be detected using spin resonance techniques. These studies have established a wide distribution of dangling-bond (DB) energy levels, spanning almost the whole semiconductor energy gap, with each DB characterized by a large on-site Coulomb energy $U \sim 0.5$ eV.[8,9] When the DB energy level falls within k_BT of the interface Fermi level, it acts as a trapping center and leads to the well known $1/f$ charge and current noise for interface conduction electrons.[10] Nevertheless at low temperatures the area density for trapping-center DBs is only a tiny fraction of the area density for *paramagnetic* DBs. For example, at $T=5$ K this fraction is only $k_BT/U \sim 10^{-3}$ (Fig. 1). As a consequence, the magnetic noise due to paramagnetic DBs is at least a factor of $U/k_BT \gg 1$ larger than mag-

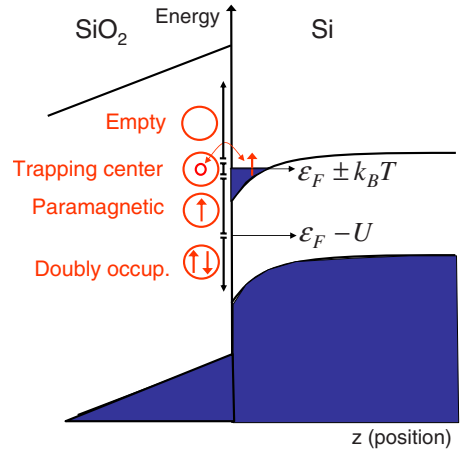

FIG. 1. (Color online) Band diagram for a Si/SiO_2 interface. Dangling bonds with energy much larger than ϵ_F are empty; DBs with energy in the interval $(\epsilon_F - k_BT, \epsilon_F + k_BT)$ are trapping centers for interface conduction electrons, responsible for charge, current, and magnetic noise. DBs with energy in the interval $(\epsilon_F - U, \epsilon_F - k_BT)$ are singly occupied (paramagnetic), and hence contribute exclusively to magnetic noise. DBs with energy less than $\epsilon_F - U$ are doubly occupied and do not contribute to any kind of noise.

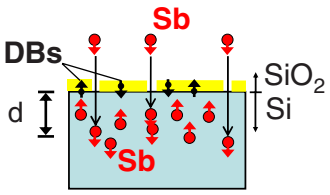

FIG. 2. (Color online) How to detect low frequency magnetic noise using electron spin resonance. A low density of antimony (Sb) donor impurities is implanted in a Si/SiO_2 sample using an ion gun, and the distribution of Sb donors is determined using secondary ion mass spectroscopy. Next, a Hahn echo decay experiment is performed on the Sb spins (Ref. 3). The Hahn echo decay envelope is directly related to magnetic noise produced by, e.g., dangling bonds at the interface, see Eq. (5).

netic noise generated by electron trapping, provided the paramagnetic DBs have a nonzero spin-flip rate (magnetic noise due to electron trapping is discussed in Appendix A).

The spin relaxation rate for dangling-bond-type defects depends crucially on the noncrystalline nature of amorphous compounds.[11–13] However, a detailed theoretical study of the magnetic field and temperature dependence of this effect has not been done. In this paper we present a general theory of dangling-bond spin-lattice relaxation in amorphous materials, and show that the noise created by the magnetic dipolar field of an ensemble of dangling bonds has the $1/f$ frequency dependence at high temperatures. We fit our theory to a recent experiment probing spin coherence of antimony donors implanted in nuclear-spin-free silicon[3] in order to estimate our model parameters.

We exploit the important relationship between phase coherence of a localized "probe" spin (e.g., the implanted Sb spins in Ref. 3) and its environmental magnetic noise (Fig. 2). The coherence decay envelope of a probe spin measured by a class of pulse spin resonance sequences is directly related to a frequency integral over magnetic noise times a filter function.[14] This allows us to interpret pulse spin resonance experiments of localized spins as sensitive detectors of magnetic noise in nanostructures. The spin qubit phase coherence is a local probe of low frequency magnetic noise. The same ideas apply equally well to experiments probing the coherent dynamics of superconducting devices.[15,16]

An important step toward this characterization was given recently, by the report of the first measurements of spin echo decay in silicon implanted with an ultralow dose of antimony donors ($\sim 10^{11}$ cm^{-2}).[3] Two samples were reported, 120 and 400 keV, with low and high implant energies, respectively. The former leads to a donor distribution closer to the interface, see Table I.

Table I provides experimental evidence that the surface leads to additional mechanisms for donor spin phase fluctuation and magnetic noise. These mechanisms seem to contribute exclusively to the phase coherence time (T_2) but not to the spin-flip time (T_1) of the Sb donors; therefore, the associated noise spectrum should be low frequency in nature (with a high frequency cutoff much smaller than the spin resonance frequency).

Here we consider the mechanisms of magnetic noise that might be playing a role in these experiments. For a Si/SiO_2 interface we show that dangling-bond spin flips play a dominant role. A DB is a paramagnetic defect usually associated with an oxygen vacancy in the Si/SiO_2 interface. These point defects are generically denoted P_b centers with chemical structure represented by $Si_3{\equiv}Si\cdot$.[8,9] There are yet no experimental or theoretical studies of spin relaxation times (T_1^{DB}) for DBs at the Si/SiO_2 interface. Nevertheless a systematic study of DB spin relaxation in bulk amorphous silicon was carried out in the 1980s.[11,13] The measured DB spin relaxation rate was found to increase as a power law on temperature, $1/T_1^{DB} \propto T^n$ with an anomalous exponent $n=2-4$ dependent on the sample preparation method. At $T=5$ K and $B=0.3$ T the typical T_1^{DB} was in the range 0.1–1 ms.[13]

TABLE I. Spin relaxation data (Ref. 3) taken at 5.2 K for antimony donor electron spins implanted in isotopically purified silicon. T_1 was measured using inversion recovery ESR, while T_2 is the $1/e$ decay of Hahn echo. For each sample, data were taken for the untreated oxidized surface (SiO_2) and for the passivated surface, treated with hydrofluoric acid in order to obtain a hydrogen terminated surface. The data clearly indicate that (1) donors close to the surface have lower spin coherence times T_2 but the same spin-flip time T_1; and (2) surface passivation leads to a sizable increment in T_2, but no change in T_1.

Sample	Interface	Peak depth (nm)	T_1 (ms)	T_2 (ms)
120 keV	Si/SiO_2	50	15±2	0.30±0.03
120 keV	Si—H	50	16±2	0.75±0.04
400 keV	Si/SiO_2	150	16±1	1.5±0.1
400 keV	Si—H	150	14±1	2.1±0.1

At first it seems puzzling that the dangling-bond spin would relax in such a short time scale at the lowest temperatures. The typical T_1 of localized electron spins in crystalline silicon (e.g., phosphorus donor impurities) is almost a thousand seconds in the same regime.[17] This happens due to the weak spin-orbit coupling in bulk crystalline silicon. However, dangling bonds in noncrystalline silicon are coupled to unstable structural defects, and this fact seems to explain their short T_1.[11,13] These structural defects behave as tunneling two-level systems strongly coupled to lattice vibrations (phonons). Each time a tunneling two-level system (TTLS) undergoes a phonon-induced transition, the DB spin feels a sudden shift in its local spin-orbit interaction, which may be quite large because the TTLS is associated with a local reordering of the atomic positions of the noncrystalline material. As a consequence, the DB spin may flip each time the TTLS switches. Remarkably, this cross-relaxation process remains effective even at zero magnetic field because it does not involve a Kramers conjugate pair (in contrast to spin flips without a simultaneous TTLS switch).

We develop this theory further in order to incorporate the exponentially wide TTLS parameter distribution typical of amorphous materials. As a result, we find that the magnetization of an initially polarized ensemble of DB spins will undergo nonexponential relaxation in time. Our theory of dangling-bond spin-lattice relaxation and magnetic noise is based on an effective Hamiltonian approach, allowing us to

draw generic conclusions about the frequency, temperature, and magnetic field dependence of spin noise in a variety of amorphous materials. For example, our results apply equally well to the magnetic noise produced by E' centers in bulk SiO_2, another well studied dangling bond. Other materials of relevance to our work are the bulk Al_2O_3 (sapphire), and Al/Al_2O_3 and Si/Si_3N_4 interfaces, whose paramagnetic dangling bonds and/or magnetic impurities are yet to be characterized experimentally.

Our results are of particular importance to magnetic flux noise in SQUIDs, whose microscopic origin is a long-standing puzzle (for a review, see Sec. IVG of Ref. 18). In Sec. VII we apply our results to calculations of flux noise due to DBs within the area enclosed by the SQUID loop, and show that this contribution might explain some of the available flux noise measurements.

It is possible to considerably reduce the dangling-bond area density using a surface passivation technique. For example, the application of hydrofluoric acid to the Si/SiO_2 surface removes dangling bonds by covering the surface with a monolayer of hydrogen atoms. Recently, Eng *et al.* fabricated a field-effect transistor using a passivated Si(111)H surface, and demonstrated record high electron mobility.[19] Nevertheless, the large density of hydrogen nuclear spins might be an important source of magnetic noise. The nuclear spins are constantly fluctuating due to their mutual dipolar coupling. In Sec. VIII we consider calculations of magnetic noise due to a hydrogen terminated Si(100)H surface. We use the same theory previously developed for Hahn echo decay of a phosphorus impurity in bulk doped natural silicon.[14,20] We show that the Hahn echo decay in a Si(100)H surface has many peculiarities, including a special crystal orientation dependence for the donor T_2 times that may be used as the fingerprint for detecting this source of noise experimentally.

II. RELATIONSHIP BETWEEN MAGNETIC NOISE AND PHASE RELAXATION IN PULSE SPIN RESONANCE EXPERIMENTS: ELECTRON SPIN AS A LOCAL PROBE OF MAGNETIC NOISE

Consider the following model Hamiltonian for the interaction of a localized spin with a noisy environment:

$$\mathcal{H} = \tfrac{1}{2}\gamma_e B\sigma_z + \hat{\boldsymbol{\eta}}(t)\cdot\boldsymbol{\sigma}. \tag{1}$$

Here $\boldsymbol{\sigma}=(\sigma_x,\sigma_y,\sigma_z)$ is the vector of Pauli matrices denoting the state of the electron spin being probed by a pulse spin resonance experiment (henceforth called the donor spin, e.g., the Sb spins in Ref. 3), $\gamma_e B$ is the spin Zeeman frequency in an applied external magnetic field B, and $\gamma_e = ge/(2m_e c)$ is a gyromagnetic ratio for the electron spin [for a group V donor impurity such as P or Sb, $\gamma_e \approx 1.76\times 10^7$ $(\mathrm{sG})^{-1}$ is close to the free electron value]. Note that Eq. (1) was divided by $\hbar$ so that energy is measured in units of frequency. Each component of the vector $\hat{\boldsymbol{\eta}}=(\hat{\eta}_x,\hat{\eta}_y,\hat{\eta}_z)$ is an operator modeling the magnetic environment (the DB or other impurity spins) surrounding the donor spin. The simplest way to describe the time evolution of the spin's magnetization $\langle\boldsymbol{\sigma}\rangle$ is the Bloch-Wangsness-Redfield approach, which assumes $\langle\boldsymbol{\sigma}\rangle$ satisfies a first order differential equation in time. The decay rate for $\langle\sigma_z\rangle$ is then given by

$$\frac{1}{T_1} = \frac{\pi}{2}\sum_{q=x,y}[\tilde{S}_q(+\gamma_e B) + \tilde{S}_q(-\gamma_e B)], \tag{2}$$

with the environmental noise spectrum defined by

$$\tilde{S}_q(\omega) = \frac{1}{2\pi}\int_{-\infty}^{\infty} e^{i\omega t}\langle\hat{\eta}_q(t)\hat{\eta}_q(0)\rangle dt. \tag{3}$$

Note that the energy relaxation time T_1 for the donor spin is determined by the noise at $\omega=\pm\gamma_e B$, that is just a statement of energy conservation. Within the Bloch-Wangsness-Redfield theory the spin's transverse magnetization ($\langle\sigma_+\rangle = \langle\sigma_x + i\sigma_y\rangle/2$) decays exponentially with the rate

$$\frac{1}{T_2^*} = \frac{1}{2T_1} + \pi\tilde{S}_z(0), \tag{4}$$

where we added an $*$ to emphasize that this rate refers to a free induction decay (FID) experiment. The Bloch-Wangsness-Redfield approach leads to a simple exponential time dependence for all spin observables. Actually this is not true in many cases of interest, including the case of a group V donor in bulk silicon where this approximation fails completely (for Si:P the observed Hahn echo decay fits well to $e^{-\tau^{2.3}}$ in many regimes).[20,34] The problem lies in the fact that the Bloch-Wangsness-Redfield theory is based on an infinite time limit approximation, that averages out finite frequency fluctuations. Note that T_2^* differs from T_1 only via static noise, $\tilde{S}_z(0)$ in Eq. (4). A large number of spin resonance sequences, most notably the Hahn echo, are able to remove static noise completely.

We may develop a theory for spin decoherence that takes into account low frequency fluctuations in the semiclassical regime $\hbar\omega \ll k_B T$, when $\tilde{S}_z(-\omega) = e^{-\hbar\omega/k_B T}\tilde{S}_z(\omega) \approx \tilde{S}_z(\omega)$. The spin coherence envelope may be calculated in the pure dephasing limit ($\hat{\eta}_x = \hat{\eta}_y = 0$), with the assumption that $\hat{\eta}_z \to \eta_z$ is distributed according to Gaussian statistics. For derivations and discussions on the applicability of this theory, we refer to Ref. 14. A similar method in the context of superconducting qubits was proposed in Ref. 16. The final result is a direct relationship between phase coherence and magnetic noise according to

$$|\langle\sigma_+(t)\rangle| = \exp\left[-\int_{-\infty}^{\infty} d\omega\tilde{S}_z(\omega)\mathcal{F}(t,\omega)\right], \tag{5}$$

with $\mathcal{F}(t,\omega)$ a filter function that depends on the particular pulse spin resonance sequence. For a free induction decay experiment ($\pi/2$-t-measure) we have

$$\mathcal{F}_{\mathrm{FID}}(t,\omega) = \frac{1}{2}\frac{\sin^2(\omega t/2)}{(\omega/2)^2}, \tag{6}$$

while for the Hahn echo ($\pi/2$-τ-π-τ-measure) the filter function becomes

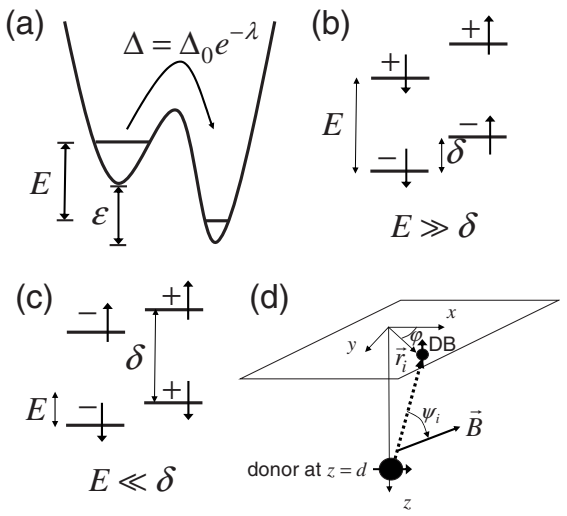

FIG. 3. (a) Effective double well potential for the tunneling two level system (TTLS). [(b) and (c)] Energy level structure for a dangling-bond (DB) spin coupled to a TTLS, for (b) $E \gg \delta$ and (c) $E \ll \delta$. (d) Coordinate system for the interaction of a dangling bond located at $\boldsymbol{r}_i$ with the donor spin. ψ_i denotes the angle formed by the donor-DB vector (dashed) and the external B field.

$$\mathcal{F}_{\mathrm{Hahn}}(2\tau,\omega) = \frac{1}{2}\frac{\sin^4(\omega\tau/2)}{(\omega/4)^2}. \tag{7}$$

Note that in the limit $t \to \infty$ Eq. (6) becomes $\pi\delta(\omega)t$, recovering the Bloch-Wangsness-Redfield result Eq. (4). The Hahn echo filter function satisfies $\mathcal{F}_{\mathrm{Hahn}}(2\tau,0)=0$, showing that it filters out terms proportional to $\tilde{S}_z(0)$ in spin evolution. This is equivalent to the well known removal of inhomogeneous broadening by the spin echo. Any pulse spin resonance sequence containing instantaneous $\pi/2$ or π pulses can be described by Eq. (5). Another important example is the class of Carr-Purcell sequences used for coherence control $(\pi/2\text{-}[\tau\text{-}\pi\text{-}\tau\text{-echo}]_{\mathrm{repeat}})$.

III. DANGLING-BOND SPIN RELAXATION: DIRECT VERSUS CROSS RELAXATION

The presence of an inversion center in crystalline Si leads to weak spin-orbit coupling and extremely long spin relaxation times. The T_1 for localized donor electrons in crystalline silicon can reach thousands of seconds at low temperatures.[17] This is in contrast to spin-lattice relaxation of dangling bonds in various forms of amorphous silicon where instead T_1^{DB} was found to range between 1 and a 100 ms at the lowest temperatures ($T=0.3-4$ K).[13] The proposed theoretical explanation was that DB spin relaxation happens due to its coupling to phonon-induced transitions of TTLSs in the amorphous material.[11] The TTLSs are thought to be structural rearrangements between groups of atoms, which can be modeled by a double well potential [see Fig. 3(a)]. The TTLS assumption is able to explain several special properties of amorphous materials at low temperatures.[21] The DB spin couples to the TTLSs either through spin-orbit or hyperfine interaction, both of which are modulated by the TTLS transition. Note that the presence of a TTLS breaks the crystal inversion symmetry.

We start by developing the theory of phonon-induced transitions for the TTLS,[22] and the associated cross relaxation of the DB spin. The Hamiltonian for a TTLS reads

$$\mathcal{H}'_{\mathrm{TTLS}} = \frac{1}{2}\begin{pmatrix} \epsilon & \Delta \\ \Delta & -\epsilon \end{pmatrix}. \tag{8}$$

The energy scale ϵ is a double well asymmetry, while $\Delta = \Delta_0 e^{-\lambda}$ is the tunneling matrix element between the states [λ is related to the barrier height and its thickness, see Fig. 3(a)]. After diagonalizing Eq. (8) we obtain $\mathcal{H}_{\mathrm{TTLS}} = \mathrm{diag}\{E/2, -E/2\}$, with $E=\sqrt{\epsilon^2+\Delta^2}$ (for notational clarity we prime the Hamiltonians in the nondiagonal basis). The coupling to phonons can be obtained by expanding the parameter ϵ to first order in the phonon strain operator,

$$\hat{u} = i\sum_{\boldsymbol{q}} \sqrt{\frac{\hbar}{2\rho V\omega_q}}|\boldsymbol{q}|(a_q e^{i\boldsymbol{q}\cdot\boldsymbol{r}} + a_q^\dagger e^{-i\boldsymbol{q}\cdot\boldsymbol{r}}), \tag{9}$$

leading to $\epsilon \to \epsilon + \epsilon'\hat{u}$. Below we average over TTLS parameters with $\epsilon \gg \Delta$, so to be consistent we must assume the deformation parameter $\Delta'=0$. Applying this expansion to Eq. (8) and transforming to the diagonal basis we get

$$\mathcal{H}_{\mathrm{TTLS\text{-}ph}} = \frac{\epsilon'\hat{u}}{2E}\begin{pmatrix} \epsilon & -\Delta \\ -\Delta & -\epsilon \end{pmatrix}. \tag{10}$$

Using Fermi's golden rule for dissipation into a phonon bath $\mathcal{H}_{\mathrm{ph}}=\Sigma_q \hbar\omega_q a_q^\dagger a_q$, we find that the transitions from $+E/2$ to $-E/2$ and vice versa are given by

$$r_+ = aE\Delta^2[n_{\mathrm{ph}}(E)+1], \tag{11}$$

$$r_- = aE\Delta^2 n_{\mathrm{ph}}(E), \tag{12}$$

with phonon occupation number

$$n_{\mathrm{ph}}(E) = \frac{1}{e^{E/k_BT}-1}. \tag{13}$$

In Eqs. (11) and (12) the parameter a depends on the material density ρ, sound velocity s, and deformation potential ϵ' [$a=(8\pi|\epsilon'|^2\hbar^4\rho s^5)^{-1}$]. The DB spin Zeeman energy is denoted by $\mathcal{H}_{\mathrm{DB}}=\hbar\gamma_e B S_z^{\mathrm{DB}}$. To simplify the notation we define $\delta \equiv \hbar\gamma_e B$ as the DB spin Zeeman energy. The coupling of the DB spin to the TTLS may be derived directly from the spin-orbit interaction $\mathcal{H}_{\mathrm{so}}=\alpha \boldsymbol{S}^{\mathrm{DB}}\cdot(\boldsymbol{E}\times\boldsymbol{p})$, where $\boldsymbol{S}^{\mathrm{DB}}$ is the DB spin operator, $\boldsymbol{p}$ is the DB orbital momentum, and $\boldsymbol{E}$ a local electric field. After averaging over the coordinate states, the resulting effective Hamiltonian becomes directly proportional to the magnetic field, a consequence of time reversal symmetry.[23] For simplicity, we assume that $\boldsymbol{E}$ is perpendicular to the interface,[24] and that the spin-orbit energy fluctuates by a certain amount $A\times\delta$ when the TTLS switches. This leads to the following effective Hamiltonian in the nondiagonal basis:

$$\mathcal{H}'_{\text{TTLS-DB}} = \frac{A\delta}{2}(S_+^{\text{DB}} + S_-^{\text{DB}})\begin{pmatrix} 1 & 0 \\ 0 & -1 \end{pmatrix}, \tag{14}$$

where $S_\pm^{\text{DB}}$ are raising and lowering operators for the DB spin. The dimensionless constant A will play the role of a small parameter in our theory. Transforming to the diagonal basis we get

$$\mathcal{H}_{\text{TTLS-DB}} = \frac{A\delta}{2E}(S_+^{\text{DB}} + S_-^{\text{DB}})\begin{pmatrix} +\epsilon & \Delta \\ \Delta & -\epsilon \end{pmatrix}. \tag{15}$$

As a result of Eq. (15), the DB-TTLS eigenstates are admixtures between spin up and spin down. We may still label the eigenstates by their spin quantum number, provided we think of $\uparrow$ ($\downarrow$) as having a large projection onto the pure spin up (down) state. The four-level structure is shown in Fig. 3(b) in the limit $E \gg \delta$ and in Fig. 3(c) for $E \ll \delta$.

The total Hamiltonian is given by

$$\mathcal{H} = \mathcal{H}_{\text{TTLS}} + \mathcal{H}_{\text{DB}} + \mathcal{H}_{\text{TTLS-DB}} + \mathcal{H}_{\text{ph}} + \mathcal{H}_{\text{TTLS-ph}}. \tag{16}$$

Note that the first three contributions denote the discrete TTLS-DB states (a four-level system), the fourth is the energy bath (a continuum of phonon states), and the fifth is the coupling between the TTLS-DB to the phonon bath. The eigenstates of the first three contributions may be calculated using perturbation theory, and the transition rates are straightforward to compute. The "direct" relaxation rate, corresponding to a DB spin flip with the TTLS state *unchanged*, is given by

$$D_{\pm\uparrow\to\pm\downarrow} = \frac{a}{4}\frac{\Delta^4 A^2}{E^2(E^2-\delta^2)^2}\delta^5[n_{\text{ph}}(\delta)+1], \tag{17}$$

with $[n_{\text{ph}}(\delta)+1]\to n_{\text{ph}}(\delta)$ for the reverse rate $D_{\pm\downarrow\to\pm\uparrow}$. Note that Eq. (17) is proportional to Δ^4, reflecting the fact that a direct spin flip may only occur together with a virtual transition to an excited orbital state.[17,23] In our case this virtual transition is a "double switch" of the TTLS, hence $D\propto\Delta^4$ [terms independent of Δ in Eq. (17) cancel exactly]; this general feature of a direct spin-flip process is referred to as "van Vleck cancellation,"[23] giving a simple explanation of why direct spin-flip rates are generally weak. Moreover, Eq. (17) vanishes at $B=0$ in accordance with time reversal symmetry (the direct process couples a Kramers pair).

The "cross-relaxation" rates, whereby the DB *spin flips simultaneously* with a TTLS switch, are given by

$$\Gamma_{-\downarrow} = a|M_+|^2(E+\delta)n_{\text{ph}}(E+\delta), \tag{18}$$

$$\Gamma_{+\uparrow} = a|M_+|^2(E+\delta)[n_{\text{ph}}(E+\delta)+1], \tag{19}$$

$$\Gamma_{-\uparrow} = a|M_-|^2(E-\delta)n_{\text{ph}}(E-\delta), \tag{20}$$

$$\Gamma_{+\downarrow} = a|M_-|^2(E-\delta)[n_{\text{ph}}(E-\delta)+1], \tag{21}$$

where the subindices label the level that the system is exiting, for example, $\Gamma_{+\uparrow}\equiv\Gamma_{+\uparrow\to-\downarrow}$. Note that the final state is obtained from the initial state by changing the sign of the TTLS and flipping the DB spin. The matrix element $M_\pm$ is defined by

$$M_\pm = \frac{A\epsilon\Delta}{E^2}[|E\pm\delta|+\delta]. \tag{22}$$

Remarkably, this cross-relaxation process is *not* a transition between Kramers conjugate states. As a result, the rates are qualitatively different from the direct process, particularly due to their magnetic field (δ) and TTLS energy (E) dependence. At low temperatures ($k_BT \ll \delta$), the direct rate always scales as $D\propto\delta^5$.[17,23] In contrast, the cross-relaxation rate has two distinct behaviors, depending whether $E\gg\delta$ or $E\ll\delta$. For $E\gg\delta$, $M_\pm\approx A\epsilon\Delta/E$, and the Γ's are independent of magnetic field. For $E\ll\delta$ we get instead $M_\pm \approx 2\delta A\epsilon\Delta/E^2$, and $\Gamma\propto\delta^3$ in contrast to the δ^5 scaling of the direct rate.

Of extreme importance to our theory is to note that whenever the energy scales E and δ are well separated, the direct rates are much smaller than the cross-relaxation rates. For $E\gg\delta$ we have $D/\Gamma\sim(\Delta/\epsilon)^2(\delta/E)^5$, while for $E\ll\delta$ we have $D/\Gamma\sim(E/\epsilon)^2(\Delta/\delta)^2$. The typical assumption for amorphous semiconductors is $\Delta\ll\epsilon$, δ and $E\approx\epsilon$.[10] In this regime the direct rates are substantially weaker than the cross-relaxation rates, except at the resonance point $E=\delta$. It is useful to list simple expressions for the cross-relaxation rates in the two most physically relevant regimes considered in this work. For low magnetic field $\delta\ll k_BT$, $E\gg\delta$ but with E/k_BT arbitrary we have simply

$$\Gamma_{\pm\uparrow} = \Gamma_{\pm\downarrow} \equiv \Gamma_\pm \approx A^2 r_\pm. \tag{23}$$

Hence when the spin-orbit coupling parameter satisfies $A \ll 1$, the cross-relaxation spin flips are much less frequent than the spin-preserving TTLS switching events. The opposite high magnetic field regime with $E\ll\delta$ and $E\ll k_BT$ with δ/k_BT arbitrary leads to

$$\Gamma_{+\uparrow} \approx \Gamma_{-\uparrow} \equiv \Gamma_\uparrow \approx 4a\frac{\delta^3A^2\Delta^2}{E^2}[n_{\text{ph}}(\delta)+1], \tag{24}$$

with the reverse rate $\Gamma_\downarrow$ given by $[n_{\text{ph}}(\delta)+1]\to n_{\text{ph}}(\delta)$. Note that these $\Gamma_{\uparrow\downarrow}$ rates are still much larger than the direct rates, since $D/\Gamma_{\uparrow\downarrow}\sim(\Delta/\delta)^2$.

Finally, we discuss how the cross-relaxation rates are affected by the presence of phonon broadening in a noncrystalline material. In this case we generalize our theory by including a complex part to the phonon spectra, $\omega_q = sq + i\gamma_{\text{ph}}$. The modified Eq. (22) becomes

$$M_\pm = \frac{A\epsilon\Delta}{E^2}\left[\frac{\delta^2+\gamma_{\text{ph}}^2/2}{\delta^2+\gamma_{\text{ph}}^2}\sqrt{(E\pm\delta)^2+\gamma_{\text{ph}}^2} + \frac{\delta}{|E\pm\delta|}\frac{(E\pm\delta)^2+\gamma_{\text{ph}}^2/2}{\sqrt{(E\pm\delta)^2+\gamma_{\text{ph}}^2}}\right]. \tag{25}$$

For amorphous Si we estimate $\gamma_{\text{ph}}\sim 0.01sq$.[25] For $E\gg\delta$, $\gamma_{\text{ph}}\sim 0.01E$ may be comparable to δ, and we see that $M_\pm$ is reduced by a factor of 2, and an additional B field dependence results.

IV. DANGLING-BOND SPIN RELAXATION: ENSEMBLE AVERAGE

In order to evaluate the ensemble averages over TTLS parameters we must first determine the time-dependent correlation function for the four-level relaxation network described in Figs. 3(b) and 3(c). Using the notation of Eq. (3), the magnetic dipolar field produced by a single DB spin maps into a c number $\hat{\eta}_z = 2h_{\rm dip}S_z^{\rm DB} \to h_{\rm dip}s_i$, with $s_i = +1$ (DB spin up) or $s_i = -1$ (DB spin down). In the four-level system notation $(+\downarrow, -\downarrow, +\uparrow, -\uparrow)$ the vector $\boldsymbol{x}$ of dipolar fields assumes the values $\boldsymbol{x} = h_{\rm dip}(-1,-1,+1,+1)$. In Appendix B we prove the convenient identity

$$S_z(t) = \langle [\eta_z(t) - \bar{\eta}_z][\eta_z(0) - \bar{\eta}_z]\rangle = \boldsymbol{x}\cdot\boldsymbol{p}(t)\cdot\boldsymbol{x}_{\boldsymbol{w}}. \quad (26)$$

Here $\boldsymbol{x}_{\boldsymbol{w}} = (x_1 w_1, x_2 w_2, \ldots)$, with w_i the equilibrium probabilities for the ith level of the DB+TTLS network. The matrix $\boldsymbol{p}(t) = e^{-\Lambda t}$ describes the occupation probability for each level, and decays according to the relaxation tensor Λ. Below we discuss the important analytic solutions for $S_z(t)$ in the limit of small spin-orbit coupling, $A \ll 1$.

A. Case $E \gg \delta$, $\delta \ll k_B T$, $E/k_B T$ arbitrary

In this regime the TTLS and cross-relaxation rates are simply related by Eq. (23). The time correlation function for the DB spin may be calculated exactly from Eq. (26), but for simplicity we show the result to lowest order in powers of A as follows:

$$S_z(t) \approx h_{\rm dip}^2[\Psi e^{-(r_+ + r_- - \bar{\Gamma})t} + (1-\Psi)e^{-\bar{\Gamma}t}], \quad (27)$$

with a visibility loss given by

$$\Psi = \frac{\tanh^2(E/2k_BT)}{\cosh^2(E/2k_BT)}A^4, \quad (28)$$

and a thermalized DB spin relaxation rate given by

$$\bar{\Gamma} = \frac{2r_-}{r_+ + r_-}\Gamma_+ + \frac{2r_+}{r_+ + r_-}\Gamma_- \approx 2aA^2\Delta^2\frac{E}{\sinh(E/k_BT)}, \quad (29)$$

where we used $\epsilon \approx E$. Interestingly, Eq. (27) shows that DB spin relaxation happens in two stages: In the first stage the DB spin decays abruptly to a small visibility loss Ψ, with a rate set by the TTLS switch. During this first stage the TTLS levels $\pm E/2$ achieve thermal equilibrium. In the second stage the DB spin relaxes fully with a much slower "thermalized" cross-relaxation rate $\bar{\Gamma}$. For $A \ll 1$ we may drop the $\Psi \propto A^4$ contribution to Eq. (27).

The theory developed above can be generalized to a single DB coupled to an ensemble of TTLSs, provided the TTLSs are not coupled to each other. In this case the rate equations (29) and (37) are generalized to a sum of rates Γ_i relating to the ith TTLS. Each exponential in Eq. (27) becomes $\sim e^{-\Sigma_i \Gamma_i t}$. This happens whenever the DB+TTLS network can be separated into disconnected four-level subspaces as in Figs. 3(b) and 3(c).

We now proceed to average over disorder realizations of the amorphous material. We assume the following two-parameter distribution:

$$P(\lambda, E) = \frac{\bar{P}v}{\lambda_{\rm max}}\left(\frac{E}{E_{\rm max}}\right)^{\alpha}, \quad (30)$$

for $\lambda \in [0, \lambda_{\rm max}]$, and $E \in [E_{\rm min}, E_{\rm max}]$; $P(\lambda, E) = 0$ otherwise. Note that the uniform distribution in λ leads to a broad distribution of TTLS tunneling parameters $\Delta = \Delta_0 e^{-\lambda}$. To our knowledge there are no estimates available for $\bar{P}, E_{\rm max}, E_{\rm min}$ close to an interface, only for bulk SiO_2. For the latter material the energy density of TTLSs per unit volume $\bar{P}$ has been estimated as $\bar{P} = 10^{20}-10^{21}$ eV^{-1} cm^{-3}, and typical values for the TTLS energy range are $E_{\rm min}/k_B \sim 0.1$ K, and $E_{\rm max}/k_B \sim 10$ K.[21] Here we introduce a parameter v with units of volume, denoting the effective range for TTLSs to couple to each DB spin (for a SiO_2 layer of 10 nm we estimate $v \sim 10^3$ nm^3). The exponent α is material dependent: While $\alpha \approx 0$ seems to be appropriate for bulk SiO_2,[21] it was found that bulk amorphous Si can be described by $\alpha = 0.1-0.4$ or $\alpha = 1.2-1.5$ depending on sample preparation method (see Ref. 13 and Sec. IV C below).

The average number of TTLSs coupled to each DB spin is given by

$$\mathcal{N} = \int d\lambda \int dE P(\lambda, E) \approx \frac{\bar{P}vE_{\rm max}}{\alpha+1}. \quad (31)$$

This is also the number of thermally activated TTLSs at high temperatures, $k_BT \gg E_{\rm max}$. For lower temperatures satisfying $E_{\rm min} \ll k_BT \ll E_{\rm max}$, Eq. (31) is divided by $\cosh^2(E/2k_BT)$, leading to

$$\mathcal{N}_T \approx \bar{P}vE_{\rm max}\left(\frac{2k_BT}{E_{\rm max}}\right)^{1+\alpha}. \quad (32)$$

This is the number of *thermally activated* TTLSs interacting with each DB spin. For extremely low temperatures $k_BT \ll E_{\rm min}$ this number will be exponentially small.

We now turn to computations of the ensemble averaged DB spin relaxation rate, $\langle\bar{\Gamma}\rangle$. At shorter times satisfying $\bar{\Gamma}_{\rm Max}t \ll 1$, the DB spin magnetization $\langle S_z(t)\rangle$ decays linearly in time.[26] The rate for this linear decay is equivalent to the $\langle 1/T_1^{\rm DB}\rangle$ rate measured for bulk amorphous silicon samples in Ref. 13. This is given by

$$\langle\bar{\Gamma}\rangle = \left\langle\frac{1}{T_1^{\rm DB}}\right\rangle = \int d\lambda \int dE P(\lambda,\epsilon)\bar{\Gamma}(\lambda,E). \quad (33)$$

At high temperatures $k_BT \gg E_{\rm max}$ Eqs. (33) and (29) lead to

$$\langle\bar{\Gamma}\rangle = aA^2\Delta_0^2 k_BT\frac{\mathcal{N}}{\lambda_{\rm max}}. \quad (34)$$

The average DB spin relaxation scales linearly with temperature times the number of TTLSs surrounding the DB.

At lower temperatures satisfying $E_{\rm min} \ll k_BT \ll E_{\rm max}$ we have instead

$$\langle \bar{\Gamma} \rangle = \frac{aA^2\Delta_0^2 \bar{P} v}{\lambda_{\max} E_{\max}^{\alpha}} (k_B T)^{2+\alpha} \int_0^{\infty} dx \frac{x^{\alpha}}{\sinh^2 x} = \frac{3aA^2\Delta_0^2 k_B T}{\lambda_{\max} 2^{1+\alpha}} \mathcal{N}_T, \tag{35}$$

showing that the DB spin relaxation rate will scale proportional to $T^{2+\alpha}$.

At the very lowest temperatures $k_B T \ll E_{\min}$ there are no thermally activated TTLSs; therefore, the mechanism of DB cross relaxation is exponentially suppressed. Here other sources of DB spin relaxation may dominate [e.g., direct relaxation as in Eq. (17)], or the DB spin may not relax at all within the characteristic time scale of the experiment.

Askew *et al.* measured average DB relaxation rates in bulk amorphous silicon at low temperatures ($T=0.3-5$ K).[13] Two different preparation methods, silicon implanted with ^{28}Si, and silicon sputtered in a substrate, led to the experimental fit $\langle \bar{\Gamma} \rangle \propto T^{2.35}$. Two other preparation methods, silicon implanted with ^{20}Ne, and silicon evaporated on a substrate led to $T^{3.3}$ and $T^{3.5}$ fits, respectively. Two different values of the magnetic field were studied (0.3 and 0.5 T), and no magnetic field dependence could be detected. The T and B dependence predicted by our model agrees with experiment provided $\alpha=0.35$ for the ^{28}Si implanted and sputtered samples, and $\alpha=1.3, 1.5$ for the ^{20}Ne implanted and the evaporated samples. It is perhaps expected that α is different for each of these because the density of TTLSs should depend on the way they were created. At high temperatures, the linear in T behavior has been observed in amorphous silicon grown by evaporation.[27]

B. Case $E \ll \delta$, $E \ll k_B T$, $\delta / k_B T$ arbitrary

From Eqs. (24) and (26) we get

$$S_z(t) \approx \frac{h_{\mathrm{dip}}^2}{\cosh^2(\delta / 2k_B T)} e^{-(\Gamma_{\uparrow}+\Gamma_{\downarrow})t}. \tag{36}$$

For $E \ll \delta$ the DB relaxation rate becomes

$$\Gamma_{\uparrow} + \Gamma_{\downarrow} \approx 4aA^2 \frac{\Delta^2}{E^2} \delta^3 \coth\left(\frac{\delta}{2k_B T}\right). \tag{37}$$

Its ensemble average is given by

$$\langle \Gamma_{\uparrow} + \Gamma_{\downarrow} \rangle \approx \frac{2aA^2}{\lambda_{\max}} \left(\frac{\Delta_0^2}{E_{\max} E_{\min}}\right) \times \left(\frac{E_{\max}}{E_{\min}}\right)^{\alpha} \left(\frac{1+\alpha}{1-\alpha}\right) \mathcal{N} \delta^3 \coth\left(\frac{\delta}{2k_B T}\right), \tag{38}$$

where we assumed $\alpha < 1$. For $\alpha \geq 1$, the prefactor in Eq. (38) is modified, but the scaling $\propto \mathcal{N} \delta^3 \coth(\delta / 2k_B T)$ remains.

C. Comparison to Reference 13

We now compare our results to the theoretical model proposed by Askew *et al.*[13] In their Eq. (5) the authors wrote the expression for $\bar{\Gamma}$ in the $E \gg \delta$ regime using free parameters D, M, C, and N. In our work these are explicitly related to microscopic parameters: $D=\epsilon' \epsilon / E$, $M=-\epsilon' \Delta / E$, $C=\epsilon/(2E)$, and $N=\Delta/(2E)$. In Ref. 13 it is claimed that when the inequality $ND/E \gg -CM/\delta$ is satisfied, the average DB relaxation rate scales as $\langle T_1^{\mathrm{DB}} \rangle^{-1} \propto T^{2+\alpha} \delta^0$ (the so called Lyo and Orbach regime after Ref. 12). When this inequality is reversed, they obtained $\langle T_1^{\mathrm{DB}} \rangle^{-1} \propto T^{4+\alpha} \delta^{-2}$ (Kurtz and Stapleton regime, Ref. 11). Nevertheless, our result shows that these parameters are related by $ND=-CM>0$, so this inequality is equivalent to $\delta \gg E$. Because Eqs. (7) and (8) of Ref. 13 are based on two conflicting approximations, $\delta \gg E$ for the matrix element squared and $\delta \ll E$ for the phonon density of states, their result needs to be corrected. We showed above that the average DB relaxation scales instead as $\delta^3 \coth(\delta / 2k_B T)$ for $\delta \gg E$ and $T^{2+\alpha} \delta^0$ for $\delta \ll E$ (the latter holds for $E_{\min} \ll k_B T \ll E_{\max}$). For high temperatures $k_B T \gg E_{\max}$ we get $T \delta^0$. The corrected results are in excellent qualitative agreement with the experimental data in Ref. 13.

Reference 13 assumes $\epsilon = \Delta = E/\sqrt{2}$ and averages E according to a density $\sim E^{\alpha}$. This is in contrast to our averaging prescription that assumes instead $\Delta = \Delta_0 e^{-\lambda}$, with $\Delta_0 < \epsilon_{\min}$ and as a consequence $\epsilon \approx E$. We assume λ is uniformly distributed and the ϵ density varies as $\sim \epsilon^{\alpha}$. This assumption is motivated by the wide distributions of TTLS relaxation rates observed in glasses, and is usually employed to explain charge and current noise in semiconductors.[10] As we show below, the broader distribution of DB relaxation times leads to $1/f$ magnetic noise and nonexponential relaxation for an ensemble of DBs.

V. MAGNETIC NOISE

The total noise power for each DB spin is independent of the specific relaxation process and may be calculated exactly using elementary Boltzman statistics. The noise must satisfy the following sum rule:

$$\int_{-\infty}^{\infty} \tilde{S}_z(\omega) d\omega = \langle \eta_z^2 \rangle - \langle \eta_z \rangle^2 = \frac{\langle h_{\mathrm{dip}}^2 \rangle}{\cosh^2(\delta / 2k_B T)}. \tag{39}$$

This shows that the noise spectrum is exponentially small in the high magnetic field regime $\delta \gg k_B T$. For the opposite regime $\delta \ll k_B T$ the total noise power is independent of temperature. However, as we show below, the spectral density $\tilde{S}_z(\omega)$ may be temperature dependent when its upper frequency cutoff is temperature dependent.

A. Case $E \gg \delta$, $\delta \ll k_B T$, $E / k_B T$ arbitrary

In order to determine the noise spectrum, we must first extract the distribution of relaxation rates $P(\bar{\Gamma})$ from Eqs. (29) and (30). Under the assumption that each DB spin is coupled to only one TTLS on average [i.e., $\mathcal{N} \sim 1$ or $\mathcal{N}_T \sim 1$, see Eqs. (31) and (32)] we have

$$P(\Gamma') = \frac{\int d\lambda \int dE P(\lambda, E) \delta(\bar{\Gamma}(\lambda, E) - \Gamma')}{\int d\lambda \int dE P(\lambda, E)}. \tag{40}$$

Note that this is normalized to 1 according to $\int d\Gamma' P(\Gamma') = 1$. It is straightforward to extend Eq. (40) to a larger number of TTLSs $E_1, E_2, \ldots$, but the explicit calculation of $P(\Gamma')$

becomes difficult. Below we will derive explicit results for the case of a DB spin coupled to a single TTLS on average.

Using Eqs. (29), (30), and (40) we may evaluate the integral over λ explicitly as follows:

$$P(\Gamma') = \frac{1}{\mathcal{N}} \int dE P(0,E) \int d\lambda \frac{\delta[\lambda - \lambda_0(E)]}{\left| \frac{d\bar{\Gamma}}{d\lambda} \right|_{\lambda=\lambda_0(E)}}$$
$$= \frac{1}{2\Gamma'} \frac{1}{\mathcal{N}} \int dE P(0,E) \theta \left[\frac{2aA^2E}{\sinh(E/k_BT)} - \Gamma' \right]. \quad (41)$$

Here $\lambda_0(E)$ is the solution of $\bar{\Gamma}(\lambda_0, E) = \Gamma'$. The step function results from the fact that the delta function will "click" only when $\lambda_0(E) \in [0, \lambda_{\max}]$, or simply $\Gamma' \leqslant 2aA^2E/\sinh(E/k_BT)$.

1. High temperature, $k_BT \gg E_{\max}$

In this case the theta function in Eq. (41) is always 1 for $\Gamma' \in [\bar{\Gamma}_{\min}, \bar{\Gamma}_{\max}]$, with $\bar{\Gamma}_{\max} = 2aA^2k_BT$ and $\bar{\Gamma}_{\min} = e^{-2\lambda_{\max}} \bar{\Gamma}_{\max}$. Therefore we have simply

$$P(\Gamma') = \frac{1}{2\lambda_{\max}\Gamma'}, \quad (42)$$

for $\Gamma' \in [\bar{\Gamma}_{\min}, \bar{\Gamma}_{\max}]$, and $P(\Gamma') = 0$ otherwise. As a check, note that $\int d\Gamma' P(\Gamma') = 1$ implies the relationship $\lambda_{\max} = \frac{1}{2} \ln\left(\frac{\bar{\Gamma}_{\max}}{\bar{\Gamma}_{\min}}\right)$, as expected.

The magnetic noise is given by

$$\tilde{S}(\omega) = \langle h_{\rm dip}^2 \rangle \int d\Gamma P(\Gamma) \frac{\Gamma/\pi}{\omega^2 + \Gamma^2} = \frac{\langle h_{\rm dip}^2 \rangle}{4\lambda_{\max}} \frac{1}{|\omega|}, \quad (43)$$

for $\bar{\Gamma}_{\min} < \omega < \bar{\Gamma}_{\max}$, and $\tilde{S}(\omega) = 0$ for $\omega > \bar{\Gamma}_{\max}$. For $\omega < \bar{\Gamma}_{\min}$ it saturates at $\tilde{S}(\bar{\Gamma}_{\min})$. Hence at the highest temperatures we have *temperature independent* magnetic $1/f$ noise.

The $1/f$ frequency dependence shows that the average magnetization of an ensemble of DB spins out of equilibrium will decay nonexponentially with time t. At intermediate times satisfying $\bar{\Gamma}_{\max}^{-1} \ll t \ll \bar{\Gamma}_{\min}^{-1}$, we may show that the time correlation function (or equivalently the ensemble average of the DB z magnetization) satisfies[10]

$$\frac{\langle S_z^{\rm DB}(t) \rangle}{\langle S_z^{\rm DB}(0) \rangle} \approx 1 - \frac{C_E + \ln(\bar{\Gamma}_{\max} t)}{2\lambda_{\max}}. \quad (44)$$

This expression is valid after neglecting terms $\mathcal{O}(1/\bar{\Gamma}_{\max} t)$. Here $C_E = 0.5772$ is the Euler-Mascheroni constant.

2. Intermediate temperature, $E_{\min} \ll k_BT \ll E_{\max}$

In this case Eq. (41) becomes

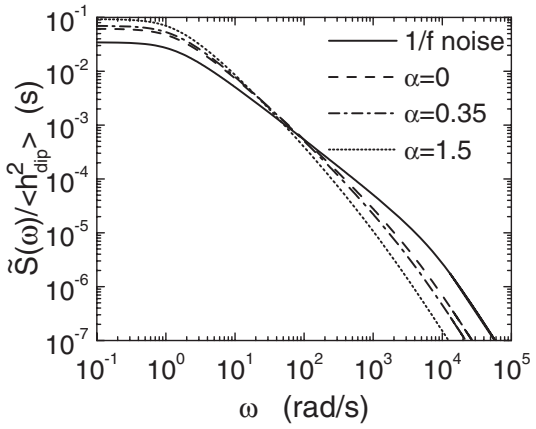

FIG. 4. Magnetic noise at intermediate temperatures $k_BT \gg \delta$ and $E_{\min} \ll k_BT \ll E_{\max}$, for $\alpha = 0, 0.35, 1.5$ (TTLS energy density exponents). The distribution of relaxation rates [Eq. (46)] contains a logarithmic correction, leading to $\tilde{S}(\omega) \propto 1/f^p$, with $p = 1.2-1.5$.

$$P(\Gamma') = \frac{1}{2\Gamma'} \frac{1+\alpha}{\lambda_{\max}} \left(\frac{k_BT}{E_{\max}}\right)^{1+\alpha} \int_0^{x_{\max}} dx x^\alpha \theta\left(\bar{\Gamma}_{\max} \frac{x}{\sinh x} - \Gamma'\right). \quad (45)$$

The upper limit of the integral is determined from $\frac{x}{\sinh x} = \Gamma'/\bar{\Gamma}_{\max}$. We solved this equation numerically, and showed that the result is well approximated by the analytic expression $x_{\max} \approx \frac{3}{2} \left| \ln\left(\frac{\Gamma'}{2\bar{\Gamma}_{\max}}\right) \right|$. Using this approximation we get

$$P(\Gamma') = \frac{1}{2\lambda_{\max}\Gamma'} \left(\frac{k_BT}{E_{\max}}\right)^{1+\alpha} \left| \frac{3}{2} \ln\left(\frac{\Gamma'}{\bar{\Gamma}_{\max}}\right) \right|^{1+\alpha}. \quad (46)$$

The distribution of relaxation rates has the same temperature dependence as the number of thermally activated TTLSs [see Eq. (32)], and possesses an interesting logarithmic correction with respect to the usual $1/\Gamma'$ behavior.

The logarithm correction in Eq. (46) increases the weight for smaller rates Γ', at the expense of decreasing the weight for higher rates. As a result the noise spectrum is better described by a $1/f^p$ relation, with $p > 1$. Figure 4 shows numerical calculations of $\tilde{S}(\omega)$ for $\alpha = 0, 0.35, 1.5$ (we assumed $\bar{\Gamma}_{\min} = 1\ {\rm s}^{-1}$ and $\bar{\Gamma}_{\max} = 10^4\ {\rm s}^{-1}$). For $\alpha = 0$, the noise is described by a $1/f^{1.2}$ fit, while for $\alpha = 1.5$ a fit of $1/f^{1.5}$ is more appropriate. Therefore at intermediate temperatures we have

$$\tilde{S}(\omega) = \frac{\langle h_{\rm dip}^2 \rangle}{4\lambda'_{\max}} \left(\frac{k_BT}{E_{\max}}\right)^{1+\alpha} \frac{1}{|\omega|^p}. \quad (47)$$

Note that $\lambda'_{\max}$ is determined from the normalization condition $\int d\omega \tilde{S}(\omega) = \langle h_{\rm dip}^2 \rangle$ for given $\bar{\Gamma}_{\max}/\bar{\Gamma}_{\min}$.

3. Extremely low temperature, $k_BT \ll E_{\min}$

In this case $\bar{\Gamma}(\lambda, E)$ is exponentially suppressed, and there will be no magnetic noise due to the DB+TTLS mechanism. If spin relaxation is dominated by the direct process [Eq.

(17)], the noise spectra may still have the $1/f$ dependence. Otherwise paramagnetic DBs may not contribute to magnetic noise at all.

4. Calculation of $\langle h_{\rm dip}^2 \rangle$

Finally, we calculate the total noise power by averaging the DB distribution over the interface plane. We choose a coordinate system with origin at the interface immediately above the donor spin. Define d as the donor depth, and r_i, ϕ_i the coordinates of the ith DB with respect to the interface [see Fig. 3(d)]. The dipolar frequency shift produced by a DB spin aligned along the same direction as the donor spin is given by

$$(h_{\rm dip})_i = \frac{\gamma_e^2 \hbar}{4(d^2 + r_i^2)^{3/2}}(1 - 3\cos^2\psi_i). \tag{48}$$

$h_{\rm dip}$ is sensitive to the orientation of the external magnetic field $\boldsymbol{B} = (\sin\theta, 0, \cos\theta)B$ with respect to the interface. This enters through

$$\cos^2\psi_i = \frac{(d\cos\theta + r_i\cos\phi_i\sin\theta)^2}{d^2 + r_i^2}. \tag{49}$$

For $\theta = 0$, the average $h_{\rm dip}^2$ over a uniform DB area density $\sigma_{\rm DB}$ is given by

$$\langle h_{\rm dip}^2 \rangle = \sigma_{\rm DB}\int_0^{2\pi} d\phi \int_0^{\infty} r dr h_{\rm dip}^2(r,\phi) = \frac{3\pi}{64}\sigma_{\rm DB}\frac{\gamma_e^4\hbar^2}{d^4}. \tag{50}$$

VI. HAHN ECHO DECAY DUE TO $1/f$ NOISE: COMPARISON TO EXPERIMENT

The discussion above concluded that the following model for the noise spectrum is valid at high temperatures ($k_B T \gg \delta$ and $k_B T \gg E_{\rm max}$):

$$\tilde{S}(\omega) = \begin{cases} C/\omega_{\rm min}, & 0 \leqslant |\omega| < \omega_{\rm min} \\ C/|\omega|, & \omega_{\rm min} \leqslant |\omega| < \omega_{\rm max} \\ 0, & \omega_{\rm max} \leqslant |\omega| < \infty. \end{cases} \tag{51}$$

The prefactor C is given by

$$C = \frac{\langle h_{\rm dip}^2 \rangle}{4\lambda_{\rm max}} \approx \frac{3\pi}{256}\frac{\sigma_{\rm DB}}{\lambda_{\rm max}}\frac{\gamma_e^4\hbar^2}{d^4}. \tag{52}$$

We may calculate the Hahn echo response due to $1/f$ noise using Eq. (5) with the filter function Eq. (7). If the interpulse time τ is neither too long (so that $c_{\rm min} = \pi\tau\omega_{\rm min}/2 < 1$) nor too short (so that $c_{\rm max} = \pi\tau\omega_{\rm max}/2 > 1$) we get

$$\langle \sigma_+(2\tau)\rangle = \exp\left(-C\tau^2\left\{\left(4\ln 2 - \frac{2}{3}c_{\rm min}^2\right) - \frac{1}{4c_{\rm max}^2}[3 - 4\cos(2c_{\rm max}) + \cos(4c_{\rm max})]\right\}\right), \tag{53}$$

after neglecting terms of order $c_{\rm min}^3$ and $1/c_{\rm max}^3$. When $c_{\rm min} \lesssim 0.1$ and $c_{\rm max} \gtrsim 10$ the echo envelope saturates and is well approximated by the simpler expression

$$\langle \sigma_+(2\tau)\rangle \approx \exp[-4\ln(2)C\tau^2], \tag{54}$$

which is independent of the low and high frequency plateaus assumed in Eq. (51).[28,29]

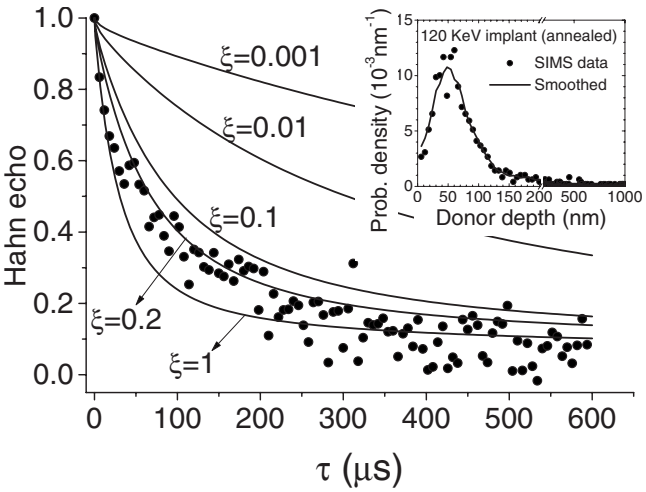

FIG. 5. Theoretical calculations (solid lines) and experimental data (circles) (Ref. 3) for Hahn echo decay of Sb donors in the 120 keV implanted sample with the Si/SiO_2 surface. The theory is in reasonable agreement with the data when the theoretical parameter $\xi \approx 0.2$ [Eq. (57)]. The inset shows the Sb donor distribution measured by secondary ion mass spectroscopy (SIMS).

In the experiment of Ref. 3, each implanted Sb donor is a probe of magnetic noise from the interface. Because the implanted profile is inhomogeneous, the parameter C is different for each layer of donors a distance d below the interface. The experimental data were taken at $\delta/k_B T = 0.3/5 = 0.06 \ll 1$. From Eq. (52) we obtain

$$\langle \sigma_+(2\tau)\rangle \approx e^{-\xi[2\pi/\chi(d)]^2}, \tag{55}$$

$$\chi(d) = \frac{6.25\ \text{nm}}{\gamma_e^2\hbar}d^2, \tag{56}$$

$$\xi = \frac{\sigma_{\rm DB} \times (\text{nm})^2}{\lambda_{\rm max}}. \tag{57}$$

In this approximation we may fit the experimental data using a single dimensionless parameter ξ, provided the distribution of Sb donors is well known.

We used Eq. (55) together with the donor distribution measured by secondary ion mass spectroscopy (SIMS) to obtain theoretical estimates of Hahn echo decay relevant to the experiment of Ref. 3. Figures 5 and 6 compare the theory with the 120 and 400 keV implanted samples, respectively, both with a Si/SiO_2 surface. A value of $\xi \approx 0.2$ for the theoretical curves seems to be consistent with the experimental data. However, in the short time range the theoretical curve seems to decay slower than the experimental data, while at longer time intervals the theory seems to decay faster. This lack of agreement may be due to deviations from the mea-

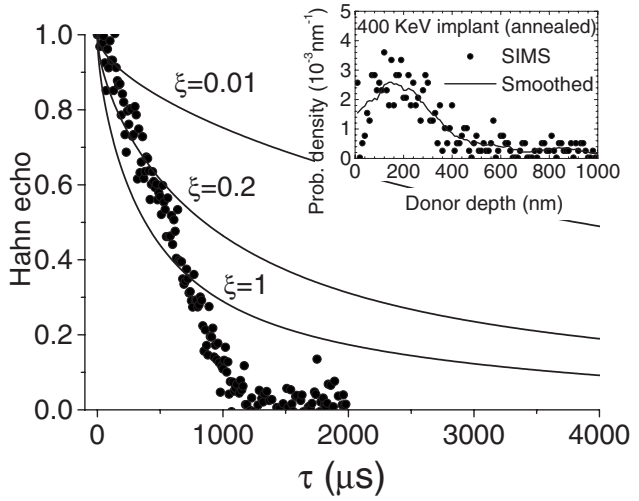

FIG. 6. Same as Fig. 5 for the 400 keV implanted sample, with the Si/SiO_2 surface. As pointed out in Ref. 3, the experimental data suffered from external field noise for $\tau > 500$ μs.

sured SIMS distribution. The ultralow donor densities were at the sensitivity threshold for the SIMS technique; hence, the donor distribution is quite noisy [see insets of Figs. 5 and 6—we used a numerically smoothed version of the SIMS-annealed data of Figs. 1(a) and 1(b) of Ref. 3]. A higher probability density near the interface could in principle explain the faster decay at shorter times, while a deeper tail in the distribution could be responsible for the slower decay at longer times.

The value for λ_{max} may be estimated from $\lambda_{max} = \frac{1}{2}\ln\left(\frac{\bar{\Gamma}_{max}}{\bar{\Gamma}_{min}}\right) \sim \frac{1}{2}\ln\left(\frac{10^6}{10^{-1}}\right) \sim 10$. Combining this with $\xi \sim 0.2$ we get $\sigma_{DB} \sim 10^{14}$ cm^{-2}.

We use Eq. (54) and the value $\xi \approx 0.2$ extracted from experiment to estimate the coherence time of a single donor located a distance d below the interface. This results in

$$T_2(d) \approx 4 \times 10^{-8}\ \mathrm{s}\left(\frac{d}{\mathrm{nm}}\right)^2, \tag{58}$$

with $T_2(d)$ inversely proportional to the square root of the DB area density. The $1/f$ noise affecting a local magnetic probe a distance d from the interface is estimated as

$$\tilde{S}(\omega) \approx \left[6.5 \times 10^{11}\ \mathrm{s}^{-2}\left(\frac{10\mathrm{nm}}{d}\right)^4\right]\frac{1}{|\omega|}, \tag{59}$$

and is directly proportional to σ_{DB}.

VII. MAGNETIC FLUX NOISE IN SQUIDs

The SQUID is probably the most sensitive probe for magnetism at the nanoscale. It consists of a superconducting loop interrupted by two insulating barriers (Josephson junctions). In this way it works as a magnetic flux-to-voltage transducer. SQUIDs are usually grown on top of a Si/SiO_2 substrate; therefore, magnetic noise due to dangling bonds within the SQUID loop will affect their performance as sensitive magnetometers.

Our results on magnetic dipolar noise are easily translated to flux noise in SQUIDs by substituting $\langle h_{dip}^2 \rangle$ for $\langle \Phi_{total}^2 \rangle$ in Sec. V above. In order to get an order of magnitude estimate for $\langle \Phi_{total}^2 \rangle$, we consider the flux produced by a single magnetic dipole moment m_0 located at the center of a disk of radius R (the area enclosed by the SQUID loop). In Gaussian units this is given by $\Phi_i = 2\pi m_0/R$. Each dangling bond contributes a dipole moment equal to $m_0 = \hbar\gamma_e/2 = \hbar e/(2m_e c)$. Assuming an area density σ_{DB} for the DBs leads to the following estimate for the mean flux squared:

$$\langle \Phi_{total}^2 \rangle \approx \pi^3 \sigma_{DB} \hbar^2 \gamma_e^2 = 2.49 \times 10^{-11} \Phi_0^2 [\sigma_{DB} \times (\mathrm{nm})^2], \tag{60}$$

where $\Phi_0 = hc/2e$ is the flux quantum. The SQUID operates at very low magnetic fields ($B \lesssim 1$ G), so the spin quantization direction is set by local inhomogeneities and is different for each DB. The angular average of spin quantization direction reduces Eq. (60) by a factor of 3. Moreover, taking account of spins close to the superconducting wire and oriented along the SQUID plane increases Eq. (60) by ~ 3.[7] As a result, Eq. (60) has the same order of magnitude as the calculation of Koch *et al.* for loop sizes 10–500 μm.[7]

At high temperatures ($k_B T \gg \delta$ and $k_B T \gg E_{max}$), the flux noise due to the presence of DBs in the plane enclosed by the SQUID loop is obtained by substituting $\langle h_{dip}^2 \rangle \to \langle \Phi_{total}^2 \rangle$ in Eq. (43). The result is

$$\tilde{S}_\Phi(\omega) = \left[\frac{\sigma_{DB} \times (\mathrm{nm})^2}{\lambda_{max}}\right] 6.2 \times 10^{-12} \frac{\Phi_0^2}{|\omega|}. \tag{61}$$

The value in brackets equals the parameter ξ used to fit our electron spin resonance (ESR) experiment (Fig. 5). Using $\xi \approx 0.2$ we get an estimate for the flux noise contribution from an untreated Si/SiO_2 substrate as follows:

$$\tilde{S}_\Phi(\omega) \approx 1.2 \times 10^{-12} \frac{\Phi_0^2}{|\omega|}. \tag{62}$$

Interestingly, this result has the same order of magnitude as the measurements of Ref. 6 using a small flux qubit as a probe of magnetic noise. A compilation of measurements of flux noise in SQUIDs was given recently by Ref. 7, where we see that $\tilde{S}(1\ \mathrm{Hz})$ lies in the range $(0.1-100) \times 10^{-12} \Phi_0^2$ for a wide variety of samples.

Note that the high temperature condition $k_B T \gg \delta$ implies $T \gg 0.1$ mK for the low magnetic fields (~ 1 G) in SQUIDs. Unfortunately, there are no estimates of E_{max} for a Si/SiO_2 interface. For bulk SiO_2 the values $E_{max} \sim 10$ K and $E_{min} \sim 0.1$ K were estimated.[21] We emphasize that Eq. (62) is the maximum value for the noise, which saturates at $k_B T \gg E_{max}$. For $k_B T < E_{max}$, Eq. (62) will be reduced by a factor $(k_B T/E_{max})^{1+\alpha}$, and the frequency dependence will change to $1/|\omega|^p$ with $p = 1.2-1.5$, see Eq. (47).

VIII. NUCLEAR SPIN NOISE FROM A HYDROGEN PASSIVATED SURFACE

Surface passivation with hydrofluoric acid drastically reduces the amount of dangling bonds. Nevertheless this oc-

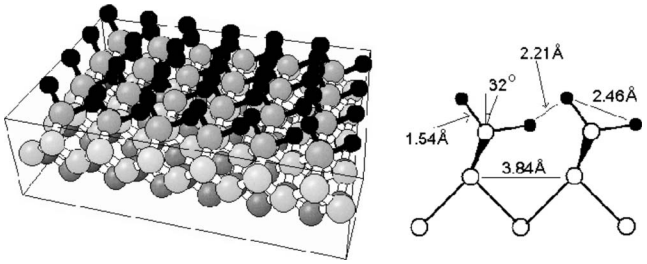

FIG. 7. A hydrogen terminated silicon surface is obtained after immersing an oxidized sample in a hydrofluoric acid solution. Here we show a Si(100)H surface with the hydrogen atoms forming a canted-row dihydride structure (Ref. 30). The SiH_2 groups form a square lattice of side $5.43/\sqrt{2}=3.84$ Å.

curs at the expense of adding a large amount of hydrogen nuclear spins. Here we investigate the magnetic noise mechanism arising due to the dipolar fluctuation of hydrogen nuclear spins at a perfect passivated Si—H surface.

It is well established that spin decoherence of donors in bulk natural silicon is dominated by nuclear spin noise from the 4.67% ^{29}Si nuclear spins.[14,20] The samples studied here[3] are known to have less than 0.1% of ^{29}Si isotopes, leading to a contribution of the order of $\frac{1}{T_2}\sim 10$ Hz. For a Si/SiO_2 sample, the fraction of oxygen isotopes with nonzero nuclear spin is even lower (0.038%); hence, oxygen nuclear spins should be a minor contributor to magnetic noise at oxidized samples.

We carry out a model calculation for the Si(100)H surface under the assumption that the hydrogen atoms are arranged in a canted-row dihydride phase with no orientation disorder, see Fig. 7.[30] The truncated Hamiltonian for a single donor electron spin interacting with the hydrogen nuclear spin lattice at the surface is given by

$$\mathcal{H}=\frac{1}{2}\gamma_e B\sigma_z-\gamma_n B\sum_i I_{iz}+\frac{1}{2}\sum_i D_i I_{iz}\sigma_z + \sum_{i\neq j} b_{ij}(I_{i+}I_{j-}-2I_{iz}I_{jz}), \tag{63}$$

where I_i is the nuclear spin operator for the hydrogen atom located at position $\boldsymbol{R}_i$ with respect to the electron [$\gamma_n=2.66\times 10^4$ (sG)$^{-1}$ is the gyromagnetic ratio for the hydrogen nuclear spin]. Note that in Eq. (63) we have neglected the nonsecular contribution of the electron-nuclear dipolar interaction. This approximation is valid only at higher external magnetic fields, $\gamma_e B\gg\sqrt{\Sigma_i D_i^2}$. For $d=10$ nm, $B>0.1$ T is necessary to satisfy this criterion. One can show numerically that the nonsecular interactions produce a loss of visibility for the Hahn echo envelope scaling as $\sim\Sigma_i D_i^2/(\gamma_e B)^2$.[31] The electron-nuclear dipolar coupling is given by

$$D_i=\frac{\gamma_n\gamma_e\hbar}{R_i^3}(1-3\cos^2\theta_i), \tag{64}$$

where θ_i is the angle between $\boldsymbol{R}_i$ and the direction of the external magnetic field. Each pair of hydrogen nuclear spins labeled by i and j are mutually coupled by the dipolar interaction

$$b_{ij}=-\frac{1}{4}\frac{\gamma_n^2\hbar}{R_{ij}^3}(1-3\cos^2\theta_{ij}), \tag{65}$$

where θ_{ij} is the angle between the B field and the vector $\boldsymbol{R}_{ij}$ linking the two nuclear spins.

The Hamiltonian equation (63) is directly mapped into the effective model Eq. (1) through the prescription $\eta_z=\Sigma_i D_i I_{iz}$. The noise spectrum [Eq. (3)] is then calculated using a "flip-flop" approximation, i.e., assuming a model that considers only flip-flop transitions between pairs of nuclear spins. In this approximation, the noise spectrum becomes[14]

$$\tilde{S}(\omega)=\sum_{i<j}\frac{b_{ij}^2\Delta_{ij}^2}{b_{ij}^2+\Delta_{ij}^2}[\delta(\omega+E_{ij})+\delta(\omega-E_{ij})], \tag{66}$$

with $\Delta_{ij}=(D_i-D_j)/4$, and $E_{ij}=2\sqrt{b_{ij}^2+\Delta_{ij}^2}$. We dropped the inhomogeneous broadening term proportional to $\delta(\omega)$ in Eq. (66) because it does not contribute to Hahn echo decay.

Using Eqs. (5) and (66) the Hahn echo envelope becomes

$$\langle\sigma_+(2\tau)\rangle=\prod_{i<j}e^{-4b_{ij}^2\Delta_{ij}^2\tau^4\,\mathrm{sinc}^4(\tau\sqrt{b_{ij}^2+\Delta_{ij}^2})}, \tag{67}$$

where $\mathrm{sinc}\,x=\sin x/x$. This result is identical to the lowest order cluster expansion derived in Ref. 20 through direct calculation of the spin echo response. Another way to derive Eq. (67) is to assume that the nuclear spin pair transitions are quasiparticle excitations with infinite lifetime.[32] Equation (67) is able to predict the Hahn echo decay without any phenomenological fitting parameter, in contrast to the traditional "Brownian motion" models developed previously.[33]

Note that the magnetic noise due to nuclear spins is a linear combination of sharp peaks (delta functions), reflecting the mesoscopic nature of the nuclear spin bath. Each delta function is a transition between discrete nuclear spin energy levels. This is in contrast to the continuous (Lorentzian) noise due to a single dangling-bond spin interacting with the phonon continuum.

In order to plot a continuous noise spectrum we represent the delta functions in Eq. (66) by normalized Gaussians with linewidth $\sigma=10^2$ s^{-1}. Note that the Hahn echo decay is independent of the particular choice of σ or the Gaussian line shape provided τ remains much smaller than $1/\sigma$ [in this case the Hahn echo envelope calculated by Eqs. (5) and (7) with a coarse grained noise spectrum is very well approximated by the zero broadening expression Eq. (67).

Figure 8 shows the nuclear spin noise spectrum from the point of view of a probe (a donor spin) lying 10 nm below the surface. Interestingly, we find that the noise spectrum is sensitive to the relative orientation of the external magnetic field with respect to the surface. The noise has a global minimum for $\theta\approx 50°$. As shown in Fig. 9, this effect translates into a variation of about 50% in the electron spin decoherence time T_2 [T_2 is obtained as the $1/e$ decay of the Hahn echo given by Eq. (67)]. This orientation dependence is surprisingly different than the one in bulk Si:P, see, e.g., Fig. 8 of Ref. 14. Figure 9 shows that T_2 is minimized when $\theta=0$ and maximized when $\theta\approx 50°$, in contrast to bulk Si:P where

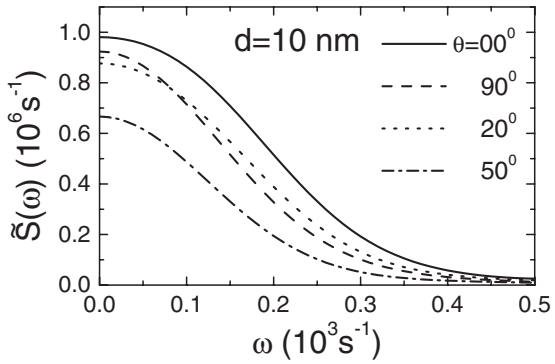

FIG. 8. Magnetic noise spectrum due to the Si(100)H surface as probed by a single donor spin 10 nm below the surface. We show the noise spectrum for four different angles θ, labeling the relative orientation of the external magnetic field with respect to the surface.

precisely the opposite was found. This special orientation dependence is the fingerprint of nuclear spin noise in a Si(100)H surface, allowing a clear identification of this mechanism in pulse spin resonance.

Figure 10 shows T_2 as a function of the donor distance from the surface. Note that we find $T_2 > 10$ ms for $d \sim 30$ nm, suggesting that this mechanism should not be playing a dominant role in the shallow implanted sample of Ref. 3 (120 keV sample). For $d > 100$ nm, T_2 is hundreds of milliseconds, so hydrogen nuclear spins are not affecting the 400 keV implanted sample either. The nuclear spin noise in a passivated surface may be further reduced by a factor of ~ 4 by using deuterium instead of hydrogen (the deuterium gyromagnetic ratio is 3.28 times smaller than hydrogen). This results in donor T_2's greater by a factor of 2.

For a perfect hydrogen passivated surface the theoretical T_2's are much longer than the values measured in Ref. 3. It is well known that chemical passivation of a Si(100) surface cannot remove all dangling bonds, in contrast to Si(111) that usually removes nearly all dangling bonds.[35] Therefore the dangling-bond mechanism might still be playing a role in the passivated samples. Repeating the experiment for the Si(111) surface could possibly yield even longer coherence times.

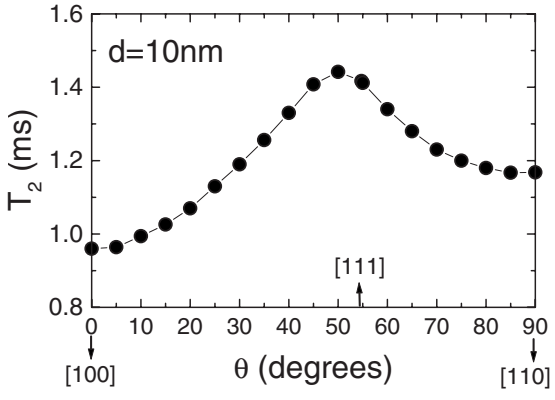

FIG. 9. Magnetic field angular dependence of T_2 for a donor spin located 10 nm below a hydrogen terminated surface. θ is the angle between the external magnetic field and the (100) direction. The resulting orientation dependence is quite distinct from the one due to ^{29}Si nuclear spins in bulk natural silicon (Refs. 14 and 34).

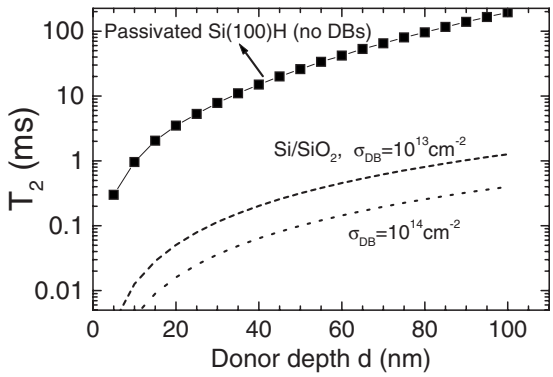

FIG. 10. Spin decoherence time T_2 as a function of the donor distance from the surface, for a passivated Si(100)H surface containing no dangling bonds (squares) and for a Si/SiO_2 interface containing a dangling-bond density equal to 10^{14} cm^{-2} [Eq. (58)].

The finite Sb density in these samples implies that the mutual interaction between donor spins (donor-donor dipolar coupling) might play a role, a mechanism of decoherence referred to as "instantaneous diffusion."[36] We have confirmed this expectation by showing that the contribution to T_2 due to instantaneous diffusion is of the order of 0.3 and 1 ms for the 120 and 400 keV samples, respectively. Therefore instantaneous diffusion might explain a fraction of the measured echo decay rates. References 36 and 37 discuss a method for completely removing the instantaneous diffusion mechanism in a doped sample.

With respect to SQUIDs, we remark that the nuclear spin flip-flop mechanism considered in this section does not contribute to magnetic flux noise (a flip-flop preserves the value of the magnetic moment for two nuclear spins, leaving the total flux unchanged). The statistical fluctuation of individual hydrogen nuclear spins (due to a finite T_1^H) should be extremely small because T_1^H is usually hundreds of seconds or more. The nuclear spin noise due to ensemble fluctuations of nuclear spins may be detected by SQUIDs under optimal circumstances, see Ref. 38.

IX. DISCUSSION

In summary, we developed a theory of magnetic noise due to spin flips of paramagnetic centers at an amorphous semiconductor-oxide interface. The mechanism of dangling-bond spin relaxation due to its interaction with tunneling two-level systems and phonons of the amorphous interface was discussed in detail. We also showed how these effects may be greatly reduced by surface passivation with hydrogen. Substituting the paramagnetic dangling bonds with a monolayer of hydrogen nuclear spins reduces the magnetic noise level by many orders of magnitude, as seen in Fig. 11. We related these results to decoherence of spin qubits in silicon as a function of their distance from the interface and flux noise in SQUID qubits.

Our work generalizes and extends the model of dangling-bond spin-lattice relaxation in amorphous materials originally proposed in Refs. 11–13. Particularly, we clarified the different temperature and magnetic field dependence as a

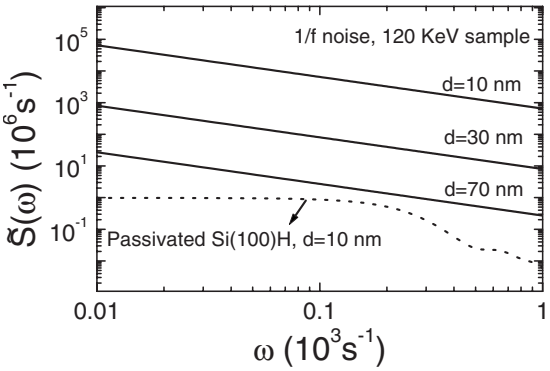

FIG. 11. Magnetic noise spectrum for the oxidized interface as probed by a single donor spin a distance d below the interface. For comparison, we show the nuclear spin noise spectrum in a hydrogen passivated surface.

function of the ratio between TTLS energy splitting E and DB spin Zeeman energy δ.

The theory of paramagnetic DB spin relaxation is significant for two recent proposals of single spin measurement based on spin-dependent recombination of conduction electrons with dangling bonds close to the Fermi level.[39,40] In these experiments the time scale T_1^{DB} sets the limit on single spin measurement fidelity. To our knowledge there is yet no experimental study of T_1^{DB} at the Si/SiO_2 surface. We propose the measurement of magnetic field and temperature dependence of DB spin relaxation at short times [Eq. (35)] and the nonexponential decay at longer times [Eq. (44)] in order to validate our theoretical results and give a full characterization of the free parameters.

Our calculations provide benchmark values for the ultimate coherence times of group V donor spin qubits implanted in an actual device structure made from nuclear-spin-free silicon. Although the longest coherence times are in principle achievable with a perfect oxidized surface *without* dangling bonds, the inevitable presence of a large density of these defects in real devices makes surface passivation an attractive alternative. Since each donor must be positioned close to an insulating interface in order to allow gate control of exchange,[2] hyperfine couplings,[41,42] as well as electron shuttling,[43] the interface effects described here will play an important role in the material optimization of silicon devices exploiting spin coherence.

Recently, ^{29}Si nuclear magnetic resonance experiments in polycrystalline silicon at room temperature were interpreted using a model of magnetic $1/f$ noise.[4] The proposed mechanism was related to the charge fluctuation of trapping centers at the surface of the microcrystals. Our work suggests that it is the spin flip of paramagnetic DBs, not trapping centers, that probably account for most of the $1/f$ noise observed in Ref. 4.

Koch *et al.* proposed a model of $1/f$ flux noise in SQUIDs based on electron hopping to localized defect sites, and concluded that a quite high trapping-center area density (5×10^{13} cm^{-2}) was required to explain flux noise in SQUID qubits.[7] Our work suggests that the spin flip of paramagnetic centers from the substrate may provide an alternative explanation, based on a more physical *paramagnetic dangling-bond density* similar to the one estimated in their work.

We remark that a C-V analysis of an unannealed Si/SiO_2 interface leads to an energy density equal to $\rho' \sim 10^{13}$ eV^{-1} cm^{-2} (see Fig. 4 of Ref. 9). This implies that the SQUID substrate is contributing at most $k_BT\rho' \sim 10^{10}$ cm^{-2} of trapping-center area density at $T=0.1-4$ K. Nevertheless, the area density for paramagnetic DBs should correlate with $U\rho' \sim 10^{13}$ cm^{-2}. The value obtained here (10^{14} cm^{-2}) is a factor of 10 higher.

Scanning tunneling microscopy experiments provide another way to estimate the trap energy density. In Ref. 44, a clean Si(100) surface was exposed to low pressure oxygen in order to produce approximately a single oxygen monolayer. When the tip to surface voltage was $\sim$1 V, 10–100 trapping centers could be detected in a 65×65 Å^2 region. This leads to an energy density in the range $10^{13}-10^{14}$ eV^{-1} cm^{-2}, higher than the C-V measurements.

The frequency and temperature dependence of flux noise in SQUIDs was measured a while ago in Ref. 5, using a wide variety of samples. These included silicon oxide substrates deliberately and not deliberately oxidized, as well as sapphire substrates. Some samples showed no temperature dependence, and the frequency dependence appeared to fit $1/f^p$, with $p=0.58-0.80$. This frequency dependence cannot be explained by our model. Nevertheless, the absence of temperature dependence may be explained by our model, provided the majority of DBs are connected to one or more thermally activated TTLS (or equivalently, $E_{\max}<k_BT$). An interesting question for future research is whether the interaction between DB spins can account for this discrepancy.

This work establishes an important connection between flux noise in SQUIDs and ESR studies of implanted donor impurities or dangling bonds. As a result, ESR characterization may play an important role in the prescreening of materials for SQUID fabrication.

ACKNOWLEDGMENTS

We acknowledge useful discussions with C. Boehme, J. Clarke, P. M. Lenahan, and T. C. Shen. We are particularly grateful to J. Bokor, C. C. Lo, S. A. Lyon, T. Schenkel, and A. M. Tyryshkin for discussions and for providing the experimental data presented in this paper. We acknowledge financial support from the Nanoelectronics Research Initiative (NRI) -Western Institute of Nanoelectronics (WIN), the National Security Agency (NSA) under MOD 713106A, NSF under Grant No. 0404208, and by the Department of Energy under Contract No. DE-AC03-76SF00098.

APPENDIX A: MAGNETIC 1/f NOISE DUE TO DANGLING-BOND CHARGE TRAPPING CENTERS

Here we consider a mechanism of magnetic noise similar to the McWhorter model of current noise in semiconductor devices, which does not involve phonons.[10]

Dangling bonds with energy close to the Fermi level act as charge trapping centers, capturing electrons from interface states. Magnetic noise occurs because each time an interface electron tunnels into the DB, it produces an effective dipolar

field in the donor spin, which is given by Eq. (48) divided by 2.

The tunneling rate for a trap located a distance z from the interface is assumed to be $\Gamma(z)=\Gamma_{\max}e^{-z/\lambda}$. Here z measures the depth of the charge trap into the SiO_2 dielectric, and $z=0$ refers to a trap at the Si/SiO_2 interface. We have $\lambda=\sqrt{\hbar^2/(2m^*E_0)}/2\sim 1$ Å, where $E_0\approx 4$ eV is half the gap difference between the two materials. $\Gamma_{\max}\sim 10^9$ s^{-1} depends on the cross section for electron capturing. Assuming a uniform distribution for z in the interval $[0,z_{\max}]$ leads to a distribution of rates equal to

$$p(\Gamma)=\frac{p(z)}{\left|\frac{d\Gamma}{dz}\right|}\approx\frac{\lambda/z_{\max}}{\Gamma}, \tag{A1}$$

for $\Gamma_{\min}<\Gamma<\Gamma_{\max}$, and zero otherwise. The noise spectrum is readily calculated as

$$\begin{aligned}\tilde{S}(\omega)&=\frac{1}{4}\langle h_{\rm dip}^2\rangle\int_{\Gamma_{\min}}^{\Gamma_{\max}}d\Gamma p(\Gamma)\frac{\Gamma/\pi}{\omega^2+\Gamma^2}\\&=\frac{3\pi}{512}\frac{\lambda}{z_{\max}}(\rho' k_B T)\frac{\gamma_e^4\hbar^2}{d^4}\frac{1}{\omega}.\end{aligned} \tag{A2}$$

Therefore we have C/ω noise with parameter $C=\lambda\langle h_{\rm dip}^2\rangle/(8z_{\max})$. In order to compare to Hahn echo decay data we define a parameter ξ similar to Eq. (57). This is given by

$$\xi=\frac{\lambda}{2z_{\max}}\rho' k_B T\ (\text{nm}^2). \tag{A3}$$

The area density for DBs with energy close to the Fermi level is estimated as $\rho' k_B T$, with $\rho'\sim 10^{13}$ cm^{-2} eV^{-1}.[9] The maximum possible value of ξ (at $T=5$ K) is estimated from $\rho' k_B T<10^{10}$ cm^{-2}. Assuming $z_{\max}\sim 10\lambda$ we get $\xi<10^{-5}$. We remark that this maximum possible value for ξ is 4 orders of magnitude smaller than the value required to explain the experimental data of Ref. 3 (see Figs. 5 and 6).

APPENDIX B: CALCULATION OF THE DB SPIN TIME-DEPENDENT CORRELATION FUNCTION

We are concerned with finite frequency fluctuations of the DB spin magnetic moment along the B field (z direction); therefore, we will describe the dissipative kinetics of the DB+TTLS network considering only diagonal density matrix elements in the Bloch-Wangsness-Redfield theory.

We define the propagator matrix $P_{ij}(t)$ as the diagonal density matrix element $\rho_{ii}(t)$ subject to the initial condition $\rho_{lm}(0)=\delta_{lj}\delta_{mj}$. This is just the probability that the DB+TTLS will be at the state i at time t given that it was at state j at time $t=0$. Note that here the index i label one of the four DB+TTLS levels $(+\downarrow,-\downarrow,+\uparrow,-\uparrow)$ [see Fig. 3(b)]. Furthermore, we define the matrix $p_{ij}(t)=P_{ij}(t)-w_i$, with $w_i=\rho_{ii}(\infty)$ the equilibrium probabilities for level i. The steady state solution is then given by $p_{ij}(t\to\infty)=0$. With this definition the rate equations for the 4×4 matrix $\boldsymbol{p}$ becomes simply

$$\frac{d}{dt}\boldsymbol{p}(t)=-\boldsymbol{\Lambda}\cdot\boldsymbol{p}(t), \tag{B1}$$

with initial condition $p_{ij}(0)=\delta_{ij}-w_i$, and a relaxation tensor $\boldsymbol{\Lambda}$ defined as follows: For $i\neq k$, $\Lambda_{ik}=-\Gamma_{k\to i}$, which is minus the rate for entering level i from level k. For $i=k$, $\Lambda_{ii}=\Sigma_{j(\neq i)}\Gamma_{i\to j}$, or the sum of rates for exiting level i. The case of our four-level system without direct transitions between Zeeman sublevels is described by

$$\boldsymbol{\Lambda}=\begin{pmatrix} r_+ +\Gamma_{+\downarrow} & -r_- & 0 & -\Gamma_{-\uparrow}\\ -r_+ & r_- +\Gamma_{-\downarrow} & -\Gamma_{+\uparrow} & 0\\ 0 & -\Gamma_{-\downarrow} & r_+ +\Gamma_{+\uparrow} & -r_-\\ -\Gamma_{+\downarrow} & 0 & -r_+ & r_- +\Gamma_{-\uparrow}\end{pmatrix}. \tag{B2}$$

The vector for equilibrium probabilities $\boldsymbol{w}=(w_{+\downarrow},w_{-\downarrow},w_{+\uparrow},w_{-\uparrow})$ is the eigenvector of $\boldsymbol{\Lambda}$ with eigenvalue zero, satisfying $\Sigma_i w_i=1$.

In the four-level system notation $(+\downarrow,-\downarrow,+\uparrow,-\uparrow)$ the vector $\boldsymbol{x}$ of dipolar fields assumes the values $\boldsymbol{x}=h_{\rm dip}(-1,-1,+1,+1)$. The correlation function becomes

$$S_z(t)=\langle[\eta_z(t)-\bar{\eta}_z][\eta_z(0)-\bar{\eta}_z]\rangle \tag{B3}$$

$$=\sum_{i,j}x_i[P_{ij}(t)-w_i]x_j w_j \tag{B4}$$

$$=\boldsymbol{x}\cdot\boldsymbol{p}(t)\cdot\boldsymbol{x}_{\boldsymbol{w}}, \tag{B5}$$

with $\boldsymbol{x}_{\boldsymbol{w}}=(x_1w_1,x_2w_2,\ldots)$. Equation (B5) together with its explicit solution $\boldsymbol{p}(t)=e^{-\boldsymbol{\Lambda}}t$ allows exact calculations of the correlation function $S_z(t)$.

*Present address: Department of Physics and Astronomy, University of Victoria, Victoria, BC, Canada V8W 3P6.

[1] I. Žutić, J. Fabian, and S. Das Sarma, Rev. Mod. Phys. **76**, 323 (2004).

[2] B. E. Kane, Nature (London) **393**, 133 (1998).

[3] T. Schenkel, J. A. Liddle, A. Persaud, A. M. Tyryshkin, S. A. Lyon, R. de Sousa, K. B. Whaley, J. Bokor, J. Shangkua, and I. Chakarov, Appl. Phys. Lett. **88**, 112101 (2006).

[4] T. D. Ladd, D. Maryenko, Y. Yamamoto, E. Abe, and K. M. Itoh, Phys. Rev. B **71**, 014401 (2005).

[5] F. C. Wellstood, C. Urbina, and J. Clarke, Appl. Phys. Lett. **50**, 772 (1987); F. C. Wellstood, Ph.D. thesis, University of Califor-

nia, 1988. Samples E_1 and E_2 had silicon oxide substrates deliberately and not deliberately oxidized, respectively; samples J_1 and K_1 had sapphire substrates.

[6] F. Yoshihara, K. Harrabi, A. O. Niskanen, Y. Nakamura, and J. S. Tsai, Phys. Rev. Lett. **97**, 167001 (2006).

[7] R. H. Koch, D. P. DiVincenzo, and J. Clarke, Phys. Rev. Lett. **98**, 267003 (2007).

[8] J. P. Campbell and P. M. Lenahan, Appl. Phys. Lett. **80**, 1945 (2002); P. M. Lenahan and J. F. Conley, Jr., J. Vac. Sci. Technol. B **16**, 2134 (1998).

[9] G. J. Gerardi, E. H. Poindexter, and P. J. Caplan, Appl. Phys. Lett. **49**, 348 (1986).

[10] Sh. Kogan, *Electronic Noise and Fluctuations in Solids* (Cambridge University Press, Cambridge, 1996).

[11] S. R. Kurtz and H. J. Stapleton, Phys. Rev. Lett. **42**, 1773 (1979); Phys. Rev. B **22**, 2195 (1980).

[12] S. K. Lyo and R. Orbach, Phys. Rev. B **22**, 4223 (1980).

[13] T. R. Askew, H. J. Stapleton, and K. L. Brower, Phys. Rev. B **33**, 4455 (1986).

[14] R. de Sousa, in *Electron Spin Resonance and Related Phenomena in Low Dimensional Structures*, TAP series, edited by Marco Fanciulli (Springer-Verlag, Berlin, to be published 2008); arXiv:cond-mat/0610716.

[15] Y. Nakamura, Y. A. Pashkin, T. Yamamoto, and J. S. Tsai, Phys. Rev. Lett. **88**, 047901 (2002).

[16] J. M. Martinis, S. Nam, J. Aumentado, K. M. Lang, and C. Urbina, Phys. Rev. B **67**, 094510 (2003).

[17] G. Feher and E. A. Gere, Phys. Rev. **114**, 1245 (1959).

[18] M. B. Weissman, Rev. Mod. Phys. **60**, 537 (1988).

[19] K. Eng, R. N. McFarland, and B. E. Kane, Appl. Phys. Lett. **87**, 052106 (2005).

[20] W. M. Witzel, R. de Sousa, and S. Das Sarma, Phys. Rev. B **72**, 161306(R) (2005).

[21] Yu. M. Galperin, V. G. Karpov, and V. I. Kozub, Adv. Phys. **38**, 669 (1989).

[22] J. Jäckle, Z. Phys. **257**, 212 (1972).

[23] J. H. Van Vleck, Phys. Rev. **57**, 426 (1940).

[24] The local electric field $\boldsymbol{E}$ has contributions from the charge accumulation layer at the interface, as well as from ligands and atomic distortions. Hence in general $\boldsymbol{E}$ has a component along the interface, which adds a term proportional to S_z^{DB} to Eq. (14). This is found to produce a small shift in the DB g factor, with no qualitative effect on T_1^{DB}.

[25] J. Fabian and P. B. Allen, Phys. Rev. Lett. **77**, 3839 (1996).

[26] Note that the short time behavior must be extracted directly from $\langle S_z^{\mathrm{DB}}(t)\rangle = \Sigma_i e^{-\Gamma_i|t|}$, which is a nonanalytic function at $t=0$. Expanding at $t=0+$ gives the correct linear decay. A different result (quadratic) is obtained from expanding the inverse Fourier transform of Eq. (43): This is incorrect because $\langle S_z^{\mathrm{DB}}(t)\rangle$ is not analytic at $t=0$.

[27] J. Gourdon, P. Fretier, and J. Pescia, J. Phys. (Paris), Lett. **42**, L21 (1981).

[28] The analogous expression for free induction decay (FID) due to $1/f$ noise is equal to

$$\langle \sigma_+(t)\rangle \approx \exp\{-Ct^2[0.9328 - \ln(\omega_{\min}t)]\}.$$

The presence of a logarithmic singularity in the exponent implies that FID is usually sensitive to the particular value chosen for the low frequency cutoff $\omega_{\min}$. This is not the case for Hahn echo decay.

[29] If $c_{\min}$ or $c_{\max}$ are outside the range of validity for Eq. (54), we may still use Eq. (54) as a lower bound on the coherence (i.e., the $\approx$ can be substituted by a $>$).

[30] J. E. Northrup, Phys. Rev. B **44**, 1419(R) (1991).

[31] N. Shenvi, R. de Sousa, and K. B. Whaley, Phys. Rev. B **71**, 224411 (2005).

[32] W. Yao, R.-B. Liu, and L. J. Sham, Phys. Rev. B **74**, 195301 (2006).

[33] J. R. Klauder and P. W. Anderson, Phys. Rev. **125**, 912 (1962); B. Herzog and E. L. Hahn, *ibid.* **103**, 148 (1956).

[34] A. M. Tyryshkin, J. J. L. Morton, S. C. Benjamin, A. Ardavan, G. A. D. Briggs, J. W. Ager, and S. A. Lyon, J. Phys.: Condens. Matter **18**, S783 (2006).

[35] E. Yablonovitch, D. L. Allara, C. C. Chang, T. Gmitter, and T. B. Bright, Phys. Rev. Lett. **57**, 249 (1986).

[36] A. M. Raitsimring, K. M. Salikhov, B. A. Umanskii, and Yu. D. Tsvetkov, Sov. Phys. Solid State **16**, 492 (1974).

[37] A. M. Tyryshkin, S. A. Lyon, A. V. Astashkin, and A. M. Raitsimring, Phys. Rev. B **68**, 193207 (2003).

[38] T. Sleator, E. L. Hahn, C. Hilbert, and J. Clarke, Phys. Rev. Lett. **55**, 1742 (1985).

[39] M. Xiao, I. Martin, E. Yablonovitch, and H. W. Jiang, Nature (London) **430**, 435 (2004).

[40] A. R. Stegner, C. Boehme, H. Huebl, M. Stutzmann, K. Lips, and M. S. Brandt, Nat. Phys. **2**, 835 (2006).

[41] L. M. Kettle, H.-S. Goan, S. C. Smith, C. J. Wellard, L. C. L. Hollenberg, and C. I. Pakes, Phys. Rev. B **68**, 075317 (2003).

[42] A. S. Martins, R. B. Capaz, and B. Koiller, Phys. Rev. B **69**, 085320 (2004).

[43] A. J. Skinner, M. E. Davenport, and B. E. Kane, Phys. Rev. Lett. **90**, 087901 (2003); M. J. Calderón, B. Koiller, X. Hu, and S. Das Sarma, *ibid.* **96**, 096802 (2006).

[44] R. H. Koch and R. J. Hamers, Surf. Sci. **181**, 333 (1987).